



Strontium modulates osteogenic activity of bone cement composed of bioactive borosilicate glass particles by activating Wnt/ β -catenin signaling pathway



Xu Cui^{a,b,1}, Yadong Zhang^{c,d,1}, Jianyun Wang^{e,1}, Chengcheng Huang^a, Yudong Wang^a, Hongsheng Yang^a, Wenlong Liu^a, Ting Wang^f, Deping Wang^b, Guocheng Wang^a, Changshun Ruan^a, Dafu Chen^{g,**}, William W. Lu^{a,h}, Wenhai Huang^b, Mohamed N. Rahaman^{i,***}, Haobo Pan^{a,*}

^a Center for Human Tissues and Organs Degeneration, Shenzhen Institutes of Advanced Technology, Chinese Academy of Science, Shenzhen, 518055, PR China

^b Schools of Materials Science and Engineering, Tongji University, Shanghai, 201804, PR China

^c Department of Orthopaedics, Shanghai Fengxian Central Hospital, South Campus of the Sixth People's Hospital Affiliated to Shanghai Jiao Tong University, Shanghai, 201499, PR China

^d Department of Orthopaedics, Fengxian Central Hospital Affiliated to Southern Medical University, Shanghai, 201499, PR China

^e Shenzhen Healthemes Biotechnology Co.Ltd, Shenzhen, 518102, PR China

^f Shenzhen Key Laboratory for Innovative Technology in Orthopaedic Trauma, Department of Orthopaedics, The University of Hong Kong-Shenzhen Hospital, University of Hong Kong, Shenzhen, 518053, PR China

^g Laboratory of Bone Tissue Engineering Beijing, Laboratory of Biomedical Materials, Beijing Research Institute of Orthopaedics and Traumatology, Beijing Jishuitan Hospital, Beijing, 100035, PR China

^h Department of Orthopaedics and Traumatology, The University of Hong Kong, Room 907, Lab Block, 21 Sassoon Road, Hong Kong SAR, PR China

ⁱ Department of Materials Science and Engineering, Missouri University of Science and Technology, MO, 65409-0340, USA

ARTICLE INFO

Keywords:

Injectable bone cement
Bioactive borosilicate glass
Strontium
Signaling pathway
Bone regeneration

ABSTRACT

There is a need for synthetic grafts to reconstruct large bone defects using minimal invasive surgery. Our previous study showed that incorporation of Sr into bioactive borate glass cement enhanced the osteogenic capacity *in vivo*. However, the amount of Sr in the cement to provide an optimal combination of physicochemical properties and capacity to stimulate bone regeneration and the underlying molecular mechanism of this stimulation is yet to be determined. In this study, bone cements composed of bioactive borosilicate glass particles substituted with varying amounts of Sr (0 mol% to 12 mol% SrO) were created and evaluated *in vitro* and *in vivo*. The setting time of the cement increased with Sr substitution of the glass. Upon immersion in PBS, the cement degraded and converted more slowly to HA (hydroxyapatite) with increasing Sr substitution. The released Sr²⁺ modulated the proliferation, differentiation, and mineralization of hBMSCs (human bone marrow mesenchymal stem cells) *in vitro*. Osteogenic characteristics were optimally enhanced with cement (designated BG6Sr) composed of particles substituted with 6mol% SrO. When implanted in rabbit femoral condyle defects, BG6Sr cement supported better peri-implant bone formation and bone-implant contact, comparing to cements substituted with 0mol% or 9mol% SrO. The underlying mechanism is involved in the activation of Wnt/ β -catenin signaling pathway in osteogenic differentiation of hBMSCs. These results indicate that BG6Sr cement has a promising combination of physicochemical properties and biological performance for minimally invasive healing of bone defects.

Peer review under responsibility of KeAi Communications Co., Ltd.

* Corresponding author.

** Corresponding author.

*** Corresponding author.

E-mail addresses: chendafu@jsthospital.org (D. Chen), rahaman@mst.edu (M.N. Rahaman), hb.pan@siat.ac.cn (H. Pan).

¹ These authors are contributed equally to this work.

<https://doi.org/10.1016/j.bioactmat.2020.02.016>

Received 5 December 2019; Received in revised form 24 February 2020; Accepted 26 February 2020

Available online 14 March 2020

2452-199X/ © 2020 Production and hosting by Elsevier B.V. on behalf of KeAi Communications Co., Ltd. This is an open access article under the CC BY-NC-ND license (<http://creativecommons.org/licenses/by-nc-nd/4.0/>).

1. Introduction

Large bone defects resulting from trauma, malignancy, infections, and congenital diseases are a common occurrence in orthopedic and craniofacial surgery [1]. The preferred treatment of large bone defects is autologous bone grafts and allografts [2]. While these treatments provide varying degrees of healing and functional restoration, they can often be lengthy, arduous, and associated with numerous drawbacks and complications, such as limited supply, donor site morbidity, possible disease transmission, immune reaction and so on [3].

Consequently, a variety of biomaterials have been developed and investigated as bone graft substitutes in animal models and clinical trials. Bioactive glasses (BG) have been successfully applied for orthopedics and dentistry, mainly for repairing osseous, cystic, tumor and periodontal defects [4–6], due to the ability to react with the body fluid, leading to the formation of a surface layer of HA that bonds strongly with bone and soft tissue [7–9]. Meanwhile, ions released of the BG into the medium during the degradation process have been shown to stimulate osteogenic and angiogenic gene expression [4–6].

As a class of more recently developed bioactive glasses, borate-based glasses are receiving considerable interest for tissue engineering applications [5]. Borate-based bioactive glasses was made by partially or fully replacing the SiO₂ content of 45S5 or 13–93 glass with B₂O₃ [7,8]. This approach resulted in the creation of bioactive borosilicate and borate glasses with a range controllable degradation rates and bioactive potential through varying the SiO₂ to B₂O₃ ratio of the glass. Studies have shown that these bioactive borosilicate and borate glasses also have the capacity to support the proliferation of osteoblasts *in vitro*, tissue infiltration in rat subcutaneous implantation model *in vivo*, bone regeneration in rabbit large segmental defects *in vivo* [10–12], and to serve as implants for local drug delivery in the treatment of osteomyelitis and regenerating bone [13,14].

To acquire a treatment with less pain, a shorter hospital stay and fewer complications, there is also a need for synthetic grafts to reconstruct large bone defects using minimally invasive surgery [15]. Our previous study had developed a novel bone cement composed of bioactive borate glass particles and an aqueous chitosan setting liquid, which offered the advantages of minimally invasive surgery [16–18]. By modulating the setting reaction between the bioactive borate glass particles and the chitosan setting liquid, a cement was created with desirable physicochemical properties, such as handling properties, mechanical strength, bioactivity and biodegradation, for potential use as injectable bone cements [16,17]. This cement was also found to provide a promising treatment for healing osteomyelitis and regenerating bone in a rabbit tibial defect model *in vivo* [18]. When loaded with the antibiotic vancomycin and implanted in a rabbit tibial defect model of osteomyelitis, the cement was found to eradicate osteomyelitis in 87% of the defects. Simultaneously, the bioactive glass particles converted into HA and stimulated new bone formation in the defects after 8 weeks of implantation [18].

Meanwhile, the ease of manufacture and compositional flexibility of glasses make bioactive glasses particularly useful as implants for bone regeneration [5]. Because of their compositional flexibility, bioactive glasses can serve as a source of many of the bone metabolic elements such as Sr, Zn, Cu, Fe and Mn. As the glass degrades *in vivo*, these elements could be *in situ* released to the surrounding tissue at a biologically acceptable rate [5]. In particular, Sr-substituted bioactive glass implants can be beneficial for bone regeneration by also providing a source for controlled local release of Sr²⁺ ions [19,20].

Sr (Strontium) can facilitate bone regeneration by stimulating osteoblastic activity and inhibiting osteoclastic resorption simultaneously [21,22]. The mechanism depends on the ability of Sr to stimulate the osteogenic gene expression of MSCs (mesenchymal stem cells), and the ALP (alkaline phosphatase) activity and OPG (osteoprotegerin) secretion of osteoblasts [23]. The expression of OPG in osteoblasts can block the interaction between the RANK (receptor activator of nuclear factor

κ B) and its ligand (RANKL, receptor Activator of Nuclear Factor-κ B Ligand), which can inhibit the activity and differentiation of osteoclasts. Besides the direct inhibitory effect on osteoclasts, Sr has the potential to exert an indirect inhibitory effect on osteoclastogenesis and bone resorption through regulation of OPG expression [24]. Sr has also been found to enhance the expression of angiogenic factors, leading to a coupling between angiogenesis and osteogenesis [25].

So in a subsequent study, the composition of the borate glass particles in the cement was modified by substituting 9 mol % SrO [26]. Assays showed that these Sr-substituted borate glass particles enhanced the osteogenic capacity of the cement *in vitro* and *in vivo*. While these results are promising, the optimal amount of Sr substitution in the bioactive glass particles to achieve a cement with a desirable combination of physicochemical properties and ability to simulate bone regeneration and the underlying molecular mechanism of this simulation is yet to be determined.

The main aim of this study was to evaluate the modulation of Sr on the physicochemical properties and osteogenic capacity of a bone cement composed of bioactive borosilicate glass and a chitosan matrix, and its underlying molecular mechanism on stimulating bone regeneration. Cements composed of the glass particles substituted with varying amounts of Sr (0–12 mol% SrO) and chitosan solution were created. The injectability, setting time, bioactivity and biodegradation of the cements were evaluated *in vitro*. The ability of Sr ions released from the cements to modulate the proliferation, differentiation and mineralization of human bone marrow stem cells (hBMSCs) was studied *in vitro*. Cements were implanted for up to 8 weeks in a rabbit femoral condyle defect model *in vivo* and evaluated for their capacity to stimulate the healing of bone defects.

2. Materials and methods

2.1. Fabrication of bioactive borosilicate glass cements

The borosilicate glass cements were composed of bioactive borosilicate glass particles dispersed in a setting liquid. Five different borosilicate glass compositions were used in the experiments (Table 1), giving 5 cement groups. The base borosilicate glass composition, designated BG, contained no SrO while the other four compositions consisted of the base borosilicate glass in which 3, 6, 9 and 12 mol% of the CaO were substituted with SrO, designated BG3Sr, BG6Sr, BG9Sr and BG12Sr, respectively.

The glasses were prepared by the conventional melt quenching route [9]. Briefly, the required quantities of H₃BO₃, CaCO₃, SiO₂, Na₂CO₃, K₂CO₃, 4MgCO₃·Mg(OH)₂·5H₂O, SrCO₃ and NaH₂PO₄·2H₂O (analytical grade; Sinopharm Chemical Reagent Co., Ltd., Shanghai, China) were heated in a platinum/rhodium crucible in air for 1–2 h at 1200 °C to form a glass melt. Then the melt was quenched between two steel plates. The resulting glass was crushed and ground to form particles. Then the glass particles were sieved through stainless steel sieves to give particles of size < 40 μm.

The setting liquid for the cements was prepared by dissolving chitosan powder in acetic acid and adding β-glycerophosphate.

Table 1

Composition of base bioactive borosilicate glass (without Sr) and Sr-substituted bioactive borosilicate glasses.

Glass designation	Mole percent							
	Na ₂ O	K ₂ O	MgO	CaO	SrO	SiO ₂	B ₂ O ₃	P ₂ O ₅
BG	6	8	8	22	0	10	44	2
BG3Sr	6	8	8	19	3	10	44	2
BG6Sr	6	8	8	16	6	10	44	2
BG9Sr	6	8	8	13	9	10	44	2
BG12Sr	6	8	8	10	12	10	44	2

Chitosan powder with deacetylation of 98% (Sinopharm Chemical Reagent Co. Ltd., Shanghai, China) was dissolved in 1.0 M acetic acid (20 g per liter). After stirring for 1 h, a solution composed of β -glycerophosphate (Sinopharm Chemical Reagent Co. Ltd., Shanghai, China) in distilled water (560 g per liter) was added to the chitosan solution (ratio of chitosan solution to β -glycerophosphate solution = 7:1 by volume). The resulting solution was stirred continuously for 1 h and stored at 4 °C for subsequent use.

Cements having a paste-like consistency were formed by mixing particles of each borosilicate glass and the setting liquid for 1.0–2.0 min in a plastic bowl and pestle. A fixed solid to liquid ratio (weight of glass to volume of setting solution) of 2.0 g per ml was used for each cement. The cement was given the same designation as the particles used in its formation (i.e., BG, BG3Sr, BG6Sr, BG9Sr and BG12Sr).

2.2. Injectability, initial setting time and mechanical strength of borosilicate glass cements

The injectability of the cement paste was tested *in vitro* using a procedure described previously [16]. The cement paste, prepared as described above, was transferred into a 5 ml syringe (Kindly Enterprise Development Group Co., Ltd, Shanghai, China) with an opening diameter of 1.7 mm and extruded by applying a force of 150 N at a crosshead speed of 5 mm min⁻¹ using a mechanical testing machine (ZQ-990LA, ZHIQU Test Machine Inc., Dongguan, China). The percent injectability (I) of the cement was determined using the equation:

$$I = [(M_0 - M)/M_0] \times 100 \quad (1)$$

where M_0 is the initial mass of the cement in the syringe, and M is mass remaining in the syringe after the extrusion. Six samples of each cement were tested and the results are expressed as a mean \pm SD.

The initial setting time of the cement pastes (prepared as described above) was determined according to methods in Refs. [16,17]. Briefly, a Teflon mold containing six holes (20 mm in diameter \times 5 mm) was placed in a water bath at 37 °C. Then the cement paste was injected into the Teflon mold cavity. The initial setting time was determined using Gilmore needles (mass = 114 g; diameter = 2.117 mm). Six samples of each cement group were tested and the results are expressed as a mean \pm SD.

The compressive strength of the each cement group after setting (equilibrated for 24 h under constant environmental conditions) was tested in a mechanical testing machine (ZQ-990LA, ZHIQU Test Machine Inc., Dongguan, China). Cylindrical samples (6 mm in diameter \times 12 mm) were tested at a crosshead speed of 1.0 mm min⁻¹. Six samples of each cement group were tested and the results are expressed as a mean \pm SD.

2.3. Degradation and bioactive potential of borosilicate glass cements *in vitro*

The degradation of the cements was evaluated as a function of soaking time in phosphate buffered saline (PBS) (GE Healthcare Life Science, Utah, USA) at 37 °C. Flaky samples of each cement (10.0 mm in diameter \times 3.0 mm) were set for 24 h and soaked in 25.1 ml PBS (calculated from the apparent surface area of the specimen according to a previous study) in polyethylene containers [27]. At each time point, the cement samples were removed, washed with distilled water and dried at 80 °C. The weight loss of the cement was taken as the difference between the initial (unreacted) mass and the mass at selected soaking time. The pH of soaking medium (PBS) was tested by a pH meter (FiveEasyPlus™, METTLER TOLEDO, Shanghai, China) after room temperature cooling. Five samples of each cement group were measured at each soaking time and the results are expressed as a mean \pm SD. The concentration of Sr²⁺ ions in the soaking medium (PBS), resulting from the degradation of the borosilicate glass particles in the cement, was measured by ICP (inductively-coupled plasma atomic emission spectroscopy) (Optima 7000DV, PerkinElmer, Waltham, USA). Five samples

in each group were tested at each soaking time, and the results are expressed as a mean \pm SD.

The conversion of borosilicate glass into hydroxyapatite (HA) in the cements after soaking in PBS was determined by XRD (X-ray diffraction) (D/max-2500VB2+/PC, Rigaku, Tokyo, Japan) using monochromatic Cu K α radiation ($\lambda = 0.15406$ nm) at a scanning rate of 8° min⁻¹ (in the range 10–80° 2 θ), and FTIR (Fourier transform infrared spectroscopy) (EQUINOXSS/HYPERION2000, Bruker Corporation, Massachusetts, Germany) in the wavenumber range 400–4000 cm⁻¹ on KBr disks. Each sample was scanned 32 times at a scan rate of 0.04 cm⁻¹. The morphological features of the cements before and after soaking in PBS were examined in a FE-SEM (field emission scanning electron microscope) (Nova NanoSEM 450, FEI, The Netherlands).

2.4. *In vitro* response of human bone marrow stem cells (hBMSCs) to borosilicate glass cements

The primary hBMSCs used in these experiments was purchased from the cell bank of Chinese Academy of Sciences at Shenzhen, China. The hBMSCs were cultured in α -MEM (Corning, NY, USA) supplemented with 10% fetal bovine serum (FBS; GIBCO, Invitrogen Pty Ltd., Thornton, Australia) plus 100 U ml⁻¹ penicillin and 100 μ g ml⁻¹ streptomycin sulfate (GIBCO, Invitrogen Pty Ltd., Thornton). When approximately 80% confluence was reached, the cells were trypsinized in 0.25% pancreatic enzymes (HyClone, Beijing, China). Cells of generations 6–8, which were cultured at 37 °C in a humidified atmosphere of 5% CO₂ and 95% air, were used for all the cell culture experiments.

2.4.1. Cytotoxicity

A Live-Dead cell staining was performed to determine the cytotoxicity of the cements coculture of hBMSCs with extracts of the cements. The hBMSCs were seeded in the medium containing each group of cement samples (1.25 cm²/ml [28]) at a density of 15,000 cells/cm². After culturing for 7 days, the cells mixed with cements were rinsed with warm PBS twice and incubated for an additional 30 min in serum-free DMEM containing 2 mM calcein acetoxymethyl ester (calcein AM; Biotium, Hayward, CA, USA) and 1 μ g/ml propidium iodide (Sigma-Aldrich, St. Louis, USA). The fluorochrome-labeled cultures on the cement samples were then rinsed with PBS and examined under an epifluorescent microscope fitted with appropriate exciter and emitter filters to detect live (green fluorescent) and dead (red fluorescent) cells.

2.4.2. Cell adhesion and proliferation

Cell adhesion were assessed by seeding 1 \times 10⁴ hBMSCs on flaky specimens (10 mm in diameter \times 3 mm) of each cement in 24-well culture plates. The cells were incubated in DMEM (Dulbecco's modified Eagle's medium) (GIBCO, Invitrogen Pty Ltd., Thornton, Australia) supplemented with 10% fetal bovine serum (FBS; GIBCO, Invitrogen Pty Ltd., Thornton, Australia). The cell cultures were maintained at 37 °C in a humidified atmosphere of 5% CO₂ and 95% air. After 7 days, the samples were removed, rinsed with PBS, and fixed with glutaraldehyde (2.5 wt%) (Sinopharm Chemical Reagent Co. Ltd., Shanghai, China) in PBS for 1–2 h. Then the samples were washed with a buffer containing 4% (w/v) sucrose (Sinopharm Chemical Reagent Co. Ltd., Shanghai, China) in PBS to remove the fixative. After post-fixed in 1% osmium tetroxide (Sinopharm Chemical Reagent Co. Ltd., Shanghai, China) in PBS and dehydrated in a graded series of ethanol (50, 70, 90, 95, and 100%), the samples were coated with gold and examined in a FE-SEM (field emission scanning electron microscope) (Nova NanoSEM 450, FEI, Netherlands).

A CCK-8 (Cell Counting Kit-8) assay (Dojindo Molecular Technologies, Inc. Washington, D.C. USA) was used to evaluate the proliferation of hBMSCs cultured on the cements. Briefly, 1 \times 10⁴ hBMSCs were seeded on each cement specimen (13 mm in diameter \times 3 mm) and cultured for 1, 3, and 7 days. Then each well was added with 360 μ L culture medium and 40 μ L CCK-8 solution at each

time point, and incubated at 37 °C for another 4 h subsequently. An aliquot of 100 µL was taken from each well and transferred to a fresh 96-well plate. The absorbance of these samples was measured at 450 nm using a spectrophotometric microplate reader (Bio-Rad 680, Berkeley, USA). The results were determined as the optical density minus the absorbance of the blank wells. Six duplicates were measured at each time point, and the results are expressed as a mean ± SD.

2.4.3. DNA quantification

The global effects of the cements on the proliferation of hBMSCs were also assessed by measuring the total cellular DNA content in cultures incubated with the cement samples (10 mm in diameter × 3 mm). Samples of each cement group were added to hBMSCs cultures (with density of 1×10^4 cells per well in a 24-well plate) and incubated for 7 and 14 days. The cultures were rinsed twice with PBS after incubation. The DNA in all wells was extracted using the TIANamp Genomic DNA kit (Tiagen Biotech, Beijing, China) according to the manufacturer's instructions. The quantification of DNA concentration in each group was measured by a UV spectrophotometer (Eppendorf, Hamburg, Germany). Six duplicates were measured at each time point, and the results are expressed as a mean ± SD.

2.4.4. Alkaline phosphatase (ALP) activity

The hBMSCs were seeded on the surface of borosilicate glass cement samples with density of 1×10^4 cells per well in a 24-well plate. After culturing for 3 days at 37 °C, the medium was replaced with a self-made osteogenic differentiation medium, which contains dexamethasone, β-glycerophosphate disodium salt hydrate, L-ascorbic acid 2-phosphate sesquimagnesium salt hydrate (Sigma-Aldrich, St. Louis, USA), to induce differentiation of hBMSCs. At 7 and 14 days of incubation, the medium was removed and the cell monolayer was washed twice with PBS. The cells were then treated with cold Triton X-100 (Sigma-Aldrich, St. Louis, USA) for 1 h under agitation to extract the ALP. Aliquots of the mixture were taken for estimation of the protein concentration. The ALP assay was performed according to the manufacturer's protocol using an ALP assay kit (Mskbio, Wuhan, China). Six duplicates were measured at each time point, and the results are expressed as a mean ± SD.

2.4.5. Alizarin Red S staining

The hBMSCs were seeded on the surface of borosilicate glass cement samples with density of 1×10^4 cells per well in a 24-well plate. After 21 days of culturing, Alizarin Red S staining of hBMSCs cultures was conducted. The culture medium was removed from each well and the cells were rinsed three times with PBS. Then 4% formaldehyde solution (Sinopharm Chemical Reagent Co. Ltd., Shanghai, China) was added to fix the hBMSCs for 30 min at room temperature. After rinsed twice with PBS, the fixed cells were stained with 1 ml of 2% Alizarin Red S working solution (Sigma-Aldrich, St. Louis, USA) and incubated for about 20 min at 37 °C. Cells were then rinsed three times and visualized under an optical microscope (Axioskop 40; Carl Zeiss, Jena, Germany). The number of mineralized nodules per well was determined from the optical images. Triplicate were measured and the results are expressed as a mean ± SD.

2.4.6. Expression of the osteogenic-related genes

The hBMSCs were seeded on the surface of borosilicate glass cement samples with density of 1×10^4 cells per well in a 24-well plate. After culturing for 7, 14 and 21 days, the hBMSCs were harvested using TRIzol reagent (Invitrogen Pty Ltd., Thornton, Australia) to extract the RNA. Then the RNA was reverse-transcribed into complementary DNA (cDNA) using a Revert Aid First Strand cDNA Synthesis Kit (Thermo Fisher Scientific, Waltham, USA). Real-time PCR was performed to examine the expression of early, middle and late osteogenic-related genes (RUNX2 (runt-related transcription factor 2), BSP (bone sialoprotein) and OCN (osteocalcin)) and glyceraldehyde-3-phosphate

dehydrogenase (GAPDH) (GeneTex, Inc. Irvine, USA) mRNA levels in the hBMSCs. The expression levels of RUNX2, BSP and OCN for each cement were standardized by the internal control levels of GAPDH. Primer sequences used for real-time PCR are shown in Table 3. Amplification was denatured for 5 min at 94 °C, followed by 30 cycles of denaturation for 1 min at 94 °C; then annealed for 30 s at 54 °C and 1 min at 72 °C. After the temperature was returned to 95 °C, the samples were stored at 4 °C overnight. These procedures were performed in a PCR machine (Eppendorf, Hamburg, Germany). Six duplicates were measured at each time point, and the results are expressed as a mean ± SD.

2.4.7. Activation of Wnt signaling pathway

For activation of Wnt signaling pathway study, hBMSCs were cultured in 6-well plate at a seeding density of 1×10^5 cells/well (5 samples for each group) and incubated with media in each group for 7 days. Wnt/β-catenin signaling pathway related genes (β-catenin, DKK1, Wnt5A) were investigated by RT-qPCR (Eppendorf, Hamburg, Germany) assay as described above, and primers sequences used in this assay were listed in Table 3. Protein expressions of the β-catenin signaling pathway was analyzed by Western blot. The total protein of hBMSCs were extracted by RIPA lysis buffer (Beyotime Biotechnology, Shanghai, China) with addition of phenylmethylsulfonyl fluoride (PMSF, Sigma-Aldrich, St. Louis, USA) and protease inhibitor cocktail (Sigma-Aldrich, St. Louis, USA). After centrifugation, the supernatant of cell lysates was collected and stored in −80 °C or used immediately for Western blot assay. Standard sodium dodecyl sulfate-polyacrylamide gel electrophoresis (SDS-PAGE) were used to separate the total proteins, which were then transferred onto a polyvinylidene difluoride (PVDF) membrane. The membranes were immersed in 5% skim milk for 1 h at room temperature to block nonspecific site, and subsequently incubated with anti-β-catenin antibody (Proteintech, Wuhan, China, 1:10000) overnight at 4 °C. The anti-GAPDH antibody (Cell Signaling Technology, 1:1000) was used as reference protein. After washing with Tris Buffered Saline with Tween-20 (TBST) for four times (5 min/time), the membranes were incubated with horseradish peroxidase (HRP)-conjugated secondary antibodies (Proteintech, Wuhan, China) for 1 h at 37 °C. Eventually, the membranes were washed with TBST for four times (5 min/time) and the protein band were detected by using a ECL-plus chemiluminescent system (Beyotime Biotechnology, Shanghai, China). AlphaEase FC software was used to analysis the quantitative densitometric of the images. Meanwhile, FH 535 (R&D Systems, USA), the signal inhibitor was used to block Wnt/β-catenin signaling pathway, and the change of Wnt/β-catenin signaling pathway related genes (β-catenin, DKK1, Wnt5A) expression were analyzed. FH 535 was dissolved in PBS containing 0.1% BSA at a concentration of 20 mM. hBMSCs was pretreated for 30 min and further incubation for 24 h with FH 535 solution (20 mM) before subsequent experiments. Wnt/β-catenin signaling pathway related genes (β-catenin, DKK1, Wnt5A) was investigated by RT-qPCR (Eppendorf, Hamburg, Germany) assay as described above.

2.5. Evaluation of borosilicate glass cement in rabbit femoral condyle defect model

2.5.1. Animal model and implantation procedure

All animal studies were performed in Shenzhen Institutes of Advanced Technology (SIAT), Chinese Academy of Sciences, in accordance with the Animal Research Committee of SIAT. A total of 18 adolescent male New Zealand white rabbits (weighing of 3.0–3.5 kg) were used in experiment. The rabbits were housed individually in stainless steel cages with wire tops in a temperature-controlled (22 °C) animal facility with a 12:12 light:dark cycle (lights on at 08:30 in the discrimination studies and 07:00 in the remaining experiments). All animals were allowed free post-operative movement with food and water ad libitum. After arrival, the animals were acclimated for 7 days

prior to the start of the study. Injection sites were shaved and cleansed with 70% ethanol and Betadine TM (povidone iodine 10%). All animals were operated under general anesthesia with intraperitoneal injection of pentobarbital sodium (0.1 ml per 100 g, Tokyo Kasei Kogyo, Tokyo, Japan).

Cement paste was implanted into the medial condyle of the femur in both hind legs. A longitudinal incision was made on the anterior surface of the femur. The inner side of the knee joint was cut to expose the femur. Then the periosteum was resected and a 5 mm pilot hole was drilled using a special 6 mm diameter burr. A ring was inserted at a depth of 10 mm to ensure the appropriate depth (10 mm) of the drill hole. A 10 ml syringe was used to inject the BG, BG6Sr and BG9Sr cement paste ($n = 16$) into the prepared bone cavity. Injection of the cement paste was conducted in a retrograde manner, from the bottom of the defect to the surface, no sooner than 6 min after the start of mixing of the cement. This cement injection procedure provided a way to fill the defect in a retrograde manner which could largely prevent significant air entrapment. This procedure also provided good filling of the bone defect and good initial contact with the defect wall. The subcutaneous tissues and skin were closed up layer by layer with silk threads after the injection of cement paste. Then an antibiotic (penicillium; Tai Yu Chemical & Pharmaceutical Co., Taiwan) at a dose of 40 mg/kg were injected subcutaneously into the rabbits for 3 days, to reduce the risk of peri-operative infection. The animals were sacrificed using an overdose of barbiturate (Mebumal; ACO Läemedel AB, Solna, Sweden) at 4 and 8 weeks postimplantation, and the implants in the medial condyle of the femur were exposed and retrieved, 8 rabbits were sacrificed at each implantation time.

2.5.2. Histological analysis

The harvested femurs was first fixed in 10% formalin (BOSTER Biological Technology co.ltd, California, USA) at room temperature for 24 h, and then dehydrated in a graded series of ethanol (50, 70, 90 and 100%). After that the undecalcified specimens were embedded in polymethyl methacrylate (PMMA). The transverse sections of the segment were cut, hand-ground and polished to a final thickness of $\sim 40 \mu\text{m}$ [29]. New bone formation at the bone–cement interface of the section was identified by Van Gieson's picrofuchsin stain. Bone tissue and cement appeared red and black, respectively. The percentage of mineralized bone in direct contact with the cement implant, referred to as the bone–implant contact (BIC) value, was measured from the stained sections.

2.5.3. Microcomputed tomography (microCT) analysis

The morphology of the reconstructed femurs was assessed using micro-CT (*In vivo* micro-CT SkyScan 1176, Bruker microCT, Belgium) in 18 μm resolution scanning mode. Images were reconstructed based on Feldkamp convolution back projection algorithm and segmented into binary images using adaptive local thresholding. The percentage of new bone volume relative to tissue volume (BV/TV) was calculated.

2.6. Statistical analysis

All quantitative data are presented as mean \pm SD. Statistical analysis was performed using one-way ANOVA and the Student's t-test, with the level of significance set at $p < 0.05$.

3. Results

Table 1 gives the compositions of the borosilicate glasses used in this study. The base borosilicate glass (without Sr), designated BG, has a CaO content of 22.0 mol %. Substitution of Sr into the glass was achieved at the expense of replacing the equivalent amount of CaO in the base glass with SrO (on a molar basis). The glass compositions containing 3, 6, 9 and 12 mol % SrO are designated BG3Sr, BG6Sr, BG9Sr and BG12Sr, respectively. Cements formed from these bioactive

Table 2

Injectability, initial setting time and compressive strength of bioactive borosilicate glass cements.

Cement designation	Injectability (%)	Initial setting time (min)	Compressive strength (MPa)
BG	95.2 \pm 0.7	10.0 \pm 1.7	23.2 \pm 1.9
BG3Sr	96.6 \pm 1.2	13.6 \pm 1.5	22.4 \pm 1.6
BG6Sr	98.0 \pm 1.6	16.3 \pm 1.5	22.9 \pm 2.1
BG9Sr	98.3 \pm 1.5	22.6 \pm 2.0	23.6 \pm 1.6
BG12Sr	98.4 \pm 1.7	26.3 \pm 2.0	20.9 \pm 1.3

Table 3

Primers used for real time polymerase chain reaction (RT-PCR) analysis.

Genes	Forward primer (5'-3')	Reverse primer (5'-3')
RUNX2	CATGAGAGCCCTCAC	AGGATAAAAAGTAGGCATGCTTG
BSP	ATGGCCTGTGCTTTCTCAATG	CTCCTCTTCTTCTTCATCAC
OCN	CATGAGAGCCCTCAC	AGAGCGACACCCTAGAC
β -Catenin	GGTCCTGTGAACTTGC	GTAATCCTGTGGCTTGTCC
DKK1	ATCATAGCACCTTGGATGGG	GACCCGTGACAAAACAGAAACC
Wnt5A	AGCCAGCTGATTCTTAATACC	GCTCAACTACATGGGACTTCTT
GAPDH	ATCCCATCACCATCTTCC	GAGTCCTTCCAGTATACCA

borosilicate glasses were given the same designation as the respective glasses.

3.1. Handling properties of bioactive borosilicate glass cements

The measured injectability, initial setting time, and the compressive strength of the cements are given in Table 2. The average injectability increased from 95.2% for the BG cement to 98.0% for the BG6Sr cement but showed little further increase for cements with higher Sr substitution. There always had a small amount of paste inevitably remained in the syringe after extrusion, which gave a practical upper limit (below 100%) for this method. Therefore all of the cements might have reached the practical upper limit [30]. Attribution to the cohesiveness of the bioactive borosilicate glass particles and the chitosan phase, no observable phase separation upon extrusion from the syringe was observed for any of the cements [31]. The initial setting time of the cements increased nearly linearly with increasing Sr content of the glass particles, from an average value of 10.0 min for the BG cement to 26.3 min for the BG12Sr cement. In comparison, the compressive strength of the cements showed little dependence on Sr substitution, with average values within a narrow range of 20.9–23.2 MPa.

3.2. In vitro degradation and bioactivity of borosilicate glass cements

Fig. 1 shows the measured weight loss of the bioactive borosilicate glass cements, the pH of the soaking medium (PBS) and the concentration of Sr^{2+} ions in PBS as a function of soaking time. The weight loss (Fig. 1a) of all the cements showed the same general trend, which increased rapidly in the first 10–15 days, and then followed by a much slower increase. However, at any given time, the weight loss decreased with increasing Sr substitution of the glass, and which reason maybe as followed: The incorporation of strontium by partial substitution of magnesium and calcium is therefore expected to occupy more space and inhibit the movement and release of other ions in glass network, and thereby reduce the dissolution rate of borosilicate BGs [19]. At 20 days, the weight loss was 38.5, 29.5, and 26%, respectively, for the BG, BG6Sr and BG12Sr cements. In comparison, at 90 days when the experiments were terminated, the weight loss was about 45, 40, and 37%, respectively, for these three cements.

The pH of the PBS (Fig. 1b) mirrored the trend in the weight loss data as a function of time but it showed a weaker dependence on the amount of Sr substitution of the glass. At any time, the pH decreased

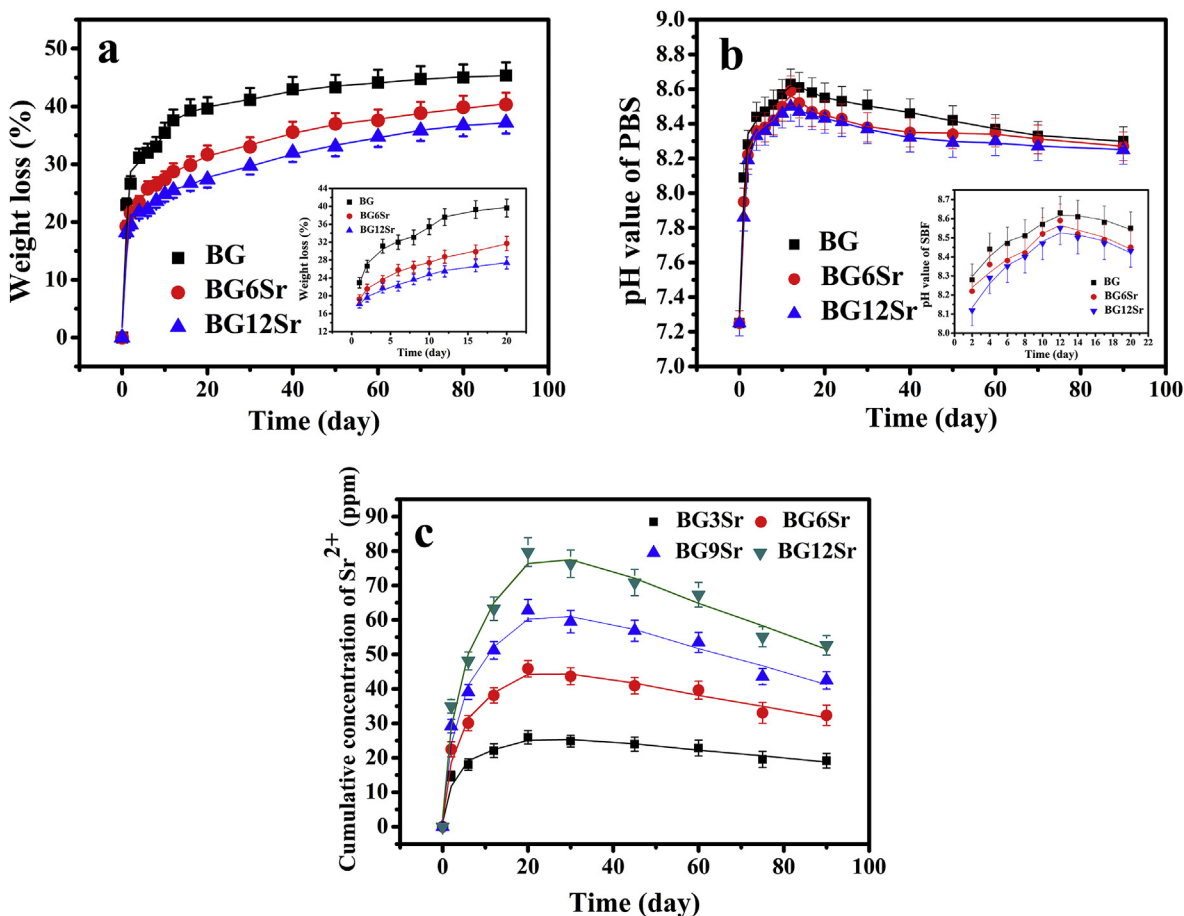


Fig. 1. (a) Weight loss of borosilicate glass cements, (b) pH of the immersion medium and (c) cumulative concentration of Sr²⁺ released into the medium as a function of immersion time in phosphate-buffered saline (PBS).

weakly with increasing Sr substitution. Starting from its initial value of 7.4, the pH increased rapidly during the first 10–15 days, reaching its highest value of 8.4–8.6 at ~12 days. Thereafter, the pH decreased slowly with time, to ~8.3 at 90 days.

The data curves for the concentration of Sr²⁺ ions released from the cements into PBS (Fig. 1c) showed the same trend with time but at any given time, the Sr²⁺ concentration increased with increasing Sr substitution of the glass. The curves increased rapidly with time, reaching a maximum value at ~20 days, after which the Sr²⁺ concentration decreased slowly. The maximum Sr²⁺ concentration (at 20 days) was 25, 45, 62.5 and 80 ppm, respectively, for the BG3Sr, BG6Sr, BG9Sr and BG12Sr cements. At 90 days, the corresponding Sr²⁺ concentration in the PBS was 20, 32.5, 42.5 and 52.5 ppm for these four cements. These data show that, starting with the BG3Sr cement, the Sr²⁺ concentration in the PBS increased approximately linearly with increasing Sr substitution of the glass.

The as-prepared cements were amorphous. After soaking of the cements for 30 days in PBS, XRD (X-ray diffraction) patterns showed a broad peak of low intensity (height) at ~30° 2θ which corresponded to the main peak in a reference HA [7,8], as shown in Fig. 2a and b for the BG and BG6Sr cement. As the soaking time increased to 60 and 90 days, the peak at ~30° 2θ became sharper and increased in intensity. There was no measurable difference in the location of this peak between the BG and BG6Sr cements but, at each time, the peak for BG cement appeared sharper and more intense than that for the BG6Sr cement. The broader and lower intensity peaks of BG6Sr cement might be an indication of a deteriorated crystallinity of as-formed HA, which may result from that Sr substitution lowered the conversion rate of the bioactive glass particles to HA [19,20]. The presence of β-

glycerophosphate or chitosan was not observed in the XRD patterns, and XRD patterns for the other cements showed a correspondingly similar trend and they are omitted for brevity.

FTIR (Fourier transform infrared) spectra of the BG and BG6Sr cements after soaking in PBS for 30, 60 and 90 days (Fig. 2c and d) showed the major vibrational bands associated with HA, and the presence of β-glycerophosphate or chitosan was not observed. These include the major band at ~1040 cm⁻¹ corresponding to the (PO₄)³⁻ ν₃ vibration and the bands at ~600 cm⁻¹ corresponding to the (PO₄)³⁻ ν₄ vibration [17]. The intensity of these two vibrational bands increased with longer immersion time, indicating an increasing amount of HA formed with time. Bands corresponding to the (CO₃)²⁻ ν₃ vibration at ~1400 cm⁻¹ and the (CO₃)²⁻ ν₂ vibration at ~873 cm⁻¹ were present in the spectra for the samples immersed in PBS, indicating the formation of a carbonate-substituted HA product [32]. There was no measurable difference in the location of the HA vibrations in the FTIR spectra of BG and BG6Sr cements. However, the vibrations in the spectrum of the BG6Sr cement were broader and less intense than those for BG cement. This indicates that Sr substitution of the glass particles lowered their conversion to HA [19,20], which is consistent with the aforementioned XRD results. FTIR spectra for the other cements showed trends correspondingly similar to those described for the BG and BG6Sr cements and they are omitted for brevity.

SEM (Scanning electron microscope) images of the surface of the BG, BG6Sr and BG12Sr cements before after soaked in PBS showed that the as-prepared cements showed a rough surface in which some BG particles and large pores are visible. After soaked in PBS for 30, 60 and 90 days, a layer of fine flake-like particles formed on the surface of the samples and covered the whole surface (Fig. 3). Taken in combination

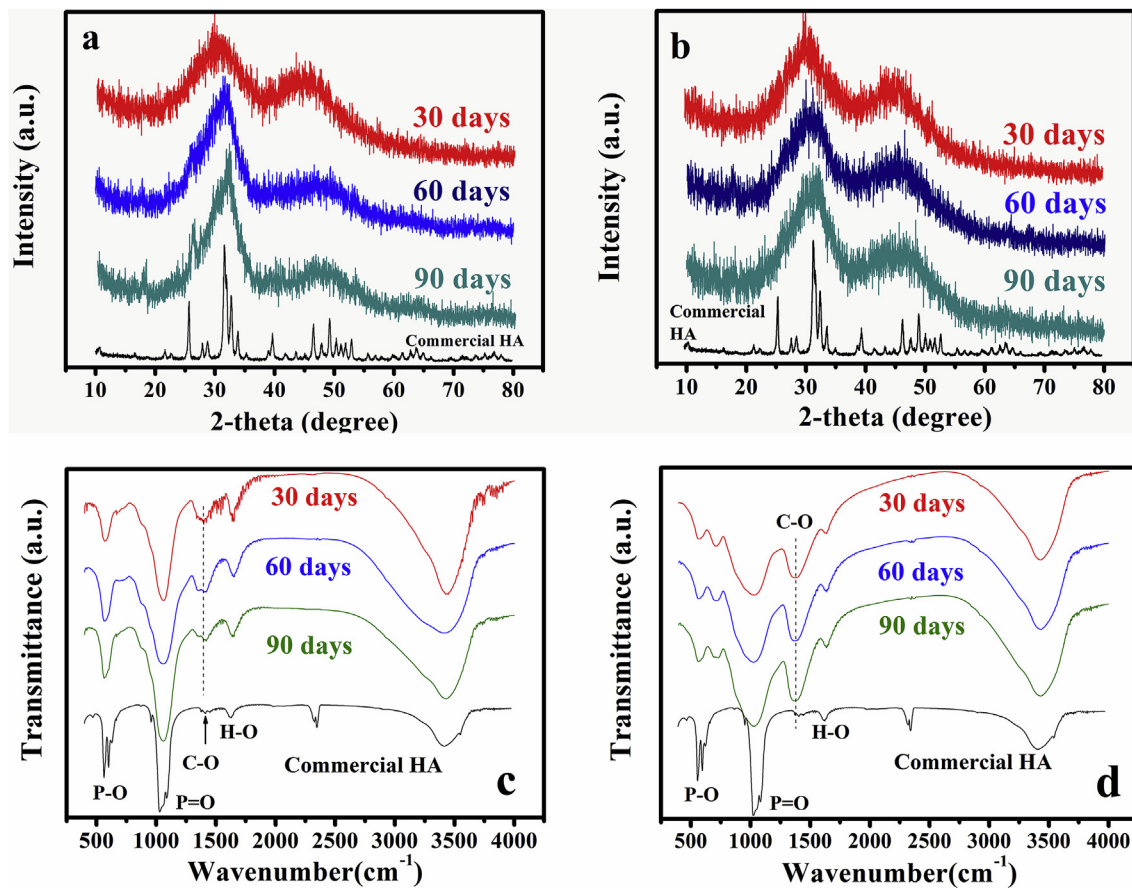


Fig. 2. X-ray diffraction patterns of (a) BG and (b) BG6Sr cement, and Fourier-transform infrared spectra of (c) BG and (d) BG6Sr cement after immersion of the cements in PBS for 30, 60 and 90 days.

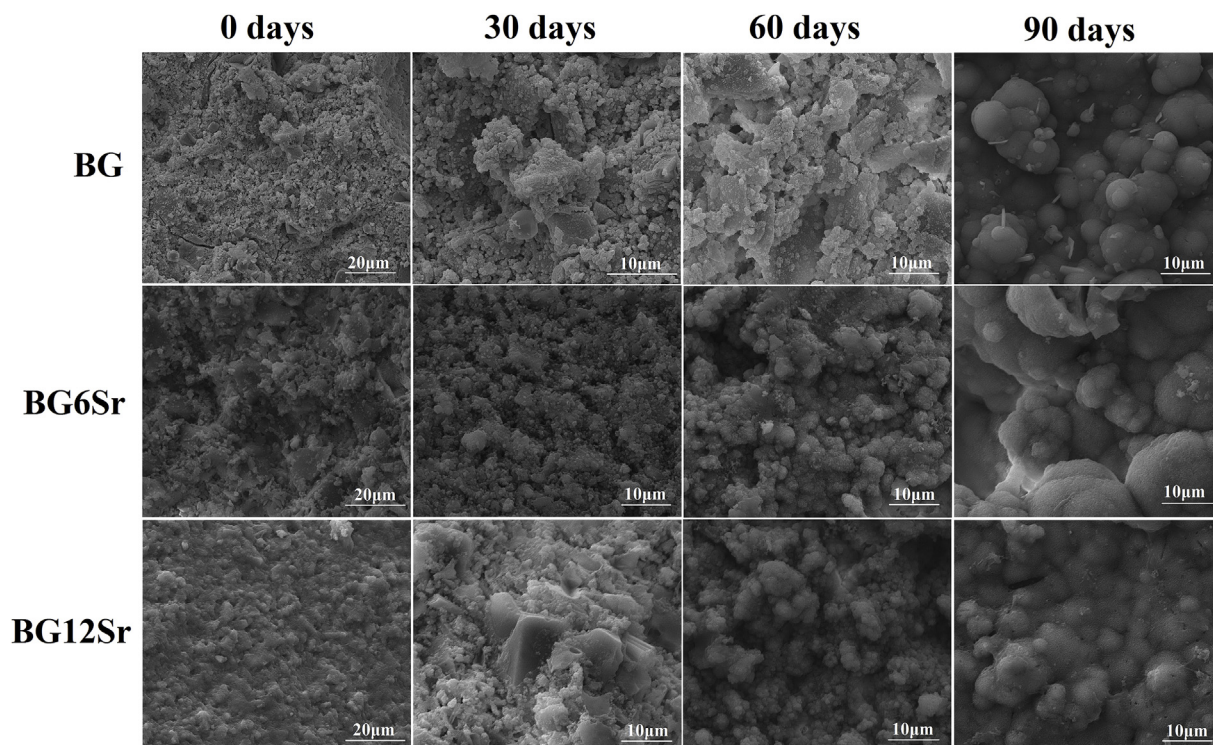


Fig. 3. Scanning electron microscope (SEM) images of the surface morphology of BG, BG6Sr and BG12Sr cements before and after immersion of the cements in PBS for 30, 60 and 90 days.

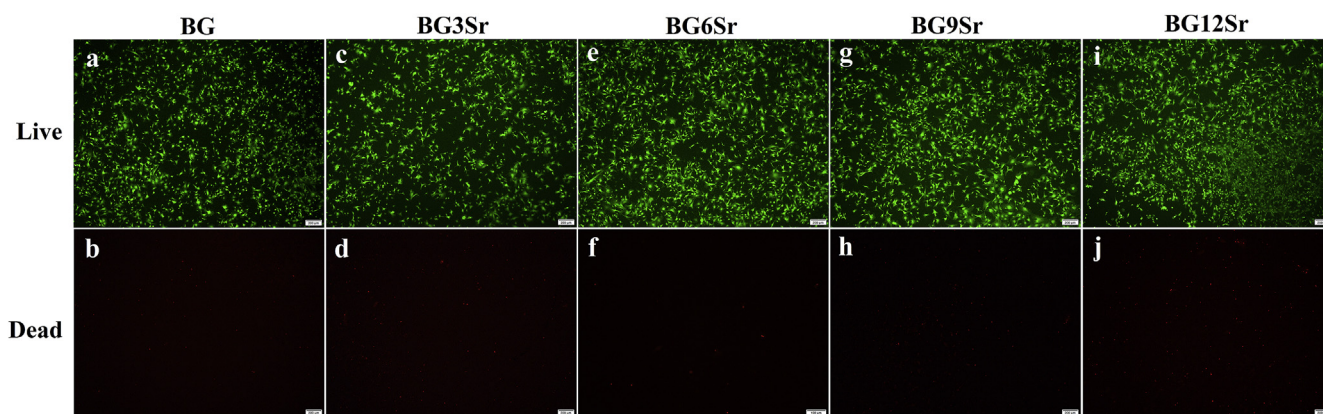


Fig. 4. Live/Dead assay after 3 days of culture period with (a, b) BG, (c, d) BG3Sr, (e, f) BG6Sr, (g, h) BG9Sr and (i, j) BG12Sr cements. Bars at 100 μm .

with the XRD and FTIR data, this particulate microstructure presumably represents an HA product formed on the surface of the cements, and the particles at the surface layer grew in size with longer immersion time and developed a more rounded morphology.

3.3. Live and dead staining of hBMSCs *in vitro*

The Live-Dead assay (Fig. 4) provided a direct observation of the proportion of living and dead cells, which can evaluate the cytotoxicity of the cement extracts to hBMSCs [19]. Live hBMSCs (stained green) suspended, proliferated and remained viable after 3 days culture with all of the cement extracts. The BG6Sr cement exhibited the least number of dead cells and the greatest number of living cells. Other groups showed a relatively higher proportion of dead cells than the BG6Sr cement.

3.4. Proliferation and ALP (alkaline phosphatase) activity of hBMSCs *in vitro*

SEM images of hBMSCs cultured for 7 days on the surface of the cements (Fig. 5) showed that the cells adhered to the cement and presented numerous lamellipodia and filopodia. All of the cements supported the proliferation of hBMSCs as measured by CCK-8 (Cell Counting Kit-8) assays (Fig. 6a). Sr substitution of the glass modulated hBMSC proliferation. Cell proliferation increased with Sr content, reached a maximum for the BG6Sr cement and decreased for the BG9Sr and BG12Sr cements. At both culture times (3 and 7 days), Sr

substitution enhanced hBMSC proliferation but the BG6Sr cement supported significantly better hBMSC proliferation than the other cements. Total DNA concentration and ALP activity of the hBMSCs cultured for 7 and 14 days on the cements are presented in Fig. 6b and c. At each culture time, the total DNA and ALP activity showed the same trend with Sr substitution as the hBMSC proliferation, i.e., the BG6Sr cement showed significantly better total DNA concentration and ALP activity than the other cements.

3.5. Biomineralization of hBMSCs *in vitro*

Alizarin red S staining was used to examine the formation of mineralized nodules by hBMSCs cultured on the cements for 21 days (Fig. 7a–e). Quantitation of mineralized nodules (Fig. 7f) showed that Sr substitution of the borosilicate glass also modulated the *in vitro* mineralization of hBMSCs. The number of mineralized nodules per well showed trends similar to those described earlier for the hBMSC proliferation and ALP activity (Fig. 6). The number of mineralized nodules was significantly higher for the Sr-substituted cements than for the BG cement, with the BG6Sr cement showing a significantly higher number of mineralized nodules per well than the other cements.

3.6. Osteogenic-related gene expression of hBMSCs

The expression levels of early, middle and late osteogenic-related genes (RUNX2, BSP and OCN, respectively) of hBMSCs incubated on the cements (Fig. 8) showed trends that were similar to the results of the *in*

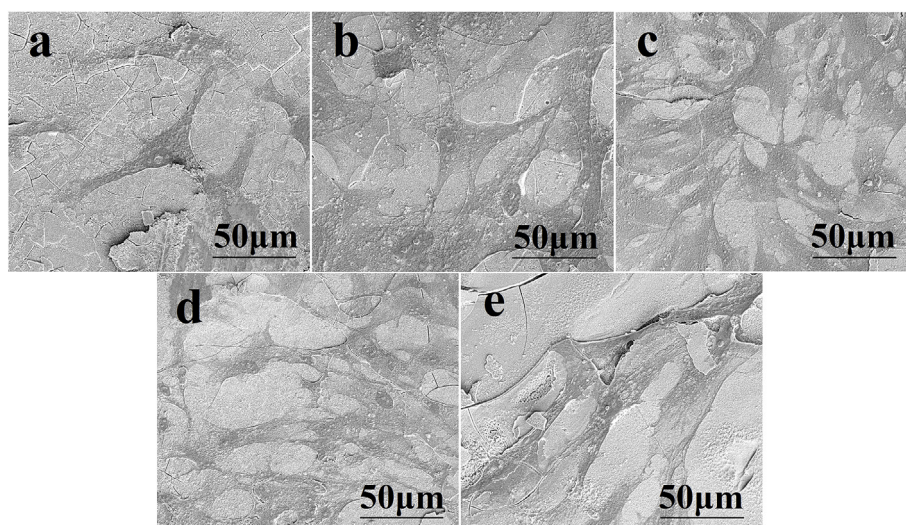


Fig. 5. SEM images showing adhesion of hBMSCs on the surface of (a) BG, (b) BG3Sr, (c) BG6Sr, (d) BG9Sr and (e) BG12Sr cements after 7 days of culture.

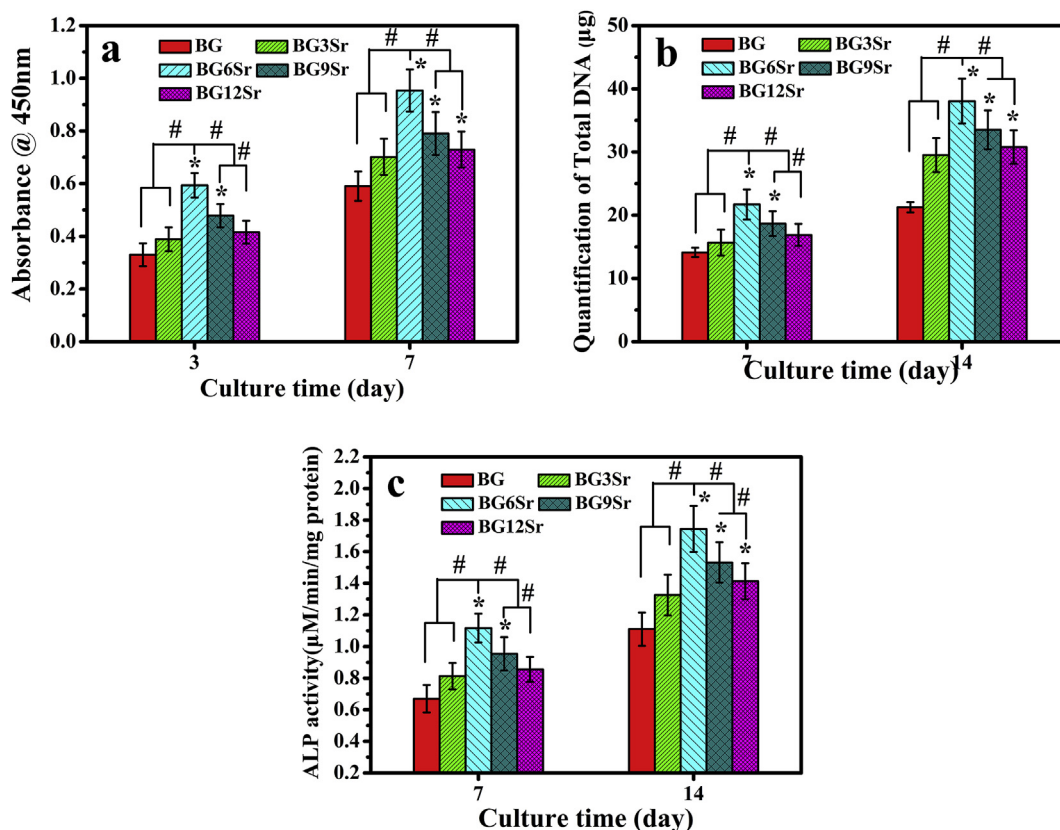


Fig. 6. (a) Proliferation of hBMSCs cultured on borosilicate glass cements for 3 and 7 days; (b) total DNA concentration and (c) ALP activity of hBMSCs cultured on borosilicate glass cements for 7 and 14 days. (Mean ± SD; n = 5; *significant difference compared with the BG group, p < 0.05; # significant difference between groups, p < 0.05).

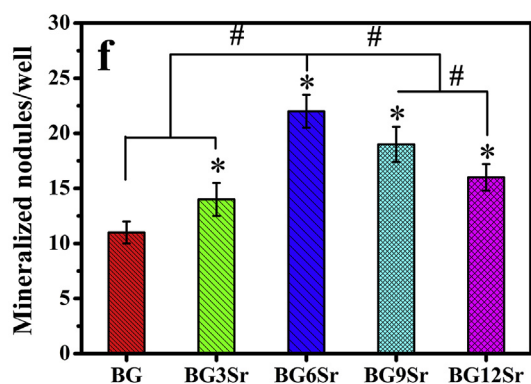
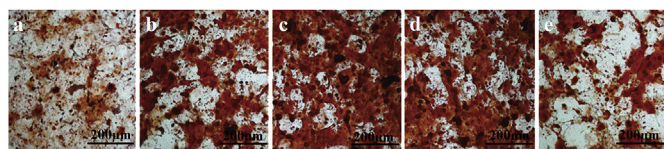


Fig. 7. Optical micrographs of (a) BG, (b) BG3Sr, (c) BG6Sr, (d) BG9Sr and (e) BG12Sr cement stained with Alizarin red S; (f) mineralized nodule formed by hBMSCs in extracts of culture media at 21 days of culture. (Mean ± SD; n = 5; *significant difference compared with the BG group, p < 0.05; # significant difference between groups, p < 0.05).

in vitro assays described earlier. When compared to the BG cement, the Sr-substituted cements stimulated enhanced expression of RUNX2 at 7 days, BSP at 14 days, and OCN at 21 days. The most significant enhancement was again shown by the BG6Sr cement.

3.7. Activation of Wnt signaling pathway

The effects of the cement groups on activation of Wnt/β-catenin determined by mRNA expression of β-catenin, DKK1 and Wnt5A, and the Western blot analysis of β-catenin protein expression were shown in Fig. 9. All the cement groups could increase the expression of β-catenin, DKK1, Wnt5A compared with control group (Fig. 9a). However, through comparison among cement groups, there was a most significant enhancement for BG6Sr cement in β-catenin and Wnt5A expression. To further determine the role of Wnt signaling pathway in cements induced osteogenesis, the cultured hBMSCs were pretreated with FH 535 (an inhibitor of Wnt signaling pathway) before the challenge of cements. After pretreated for 30 min and further incubation for 24 h with FH 535 (20 µM), the expression of β-catenin, DKK1, Wnt5A compared with control group was completely blocked (Fig. 9b). Western blot analysis (Fig. 9c and d) indicated that the protein expression of β-catenin in Sr-substituted cements were significantly higher than BG cement, whereas there were no significant differences between BG cement and control group.

3.8. Histomorphometric analysis of bone regeneration *in vivo*

The bone – cement interface in the rabbit femoral defects after the implantation of the BG, BG6Sr and BG9Sr cements for 4 and 8 weeks was further assessed using histomorphometric analysis (Fig. 10a–d). Images for the BG9Sr cement are omitted for brevity. As showed in Van Gieson's picrofuchsin stained sections, none of the cements had the signs of rejection, necrosis or infection after implanted, which indicated its well-toleration into the defect sites. At 4 weeks, there was only a small amount of newly formed bone (yellow arrowhead) and large gaps were apparent around the BG cement (designated C) (Fig. 10a). In

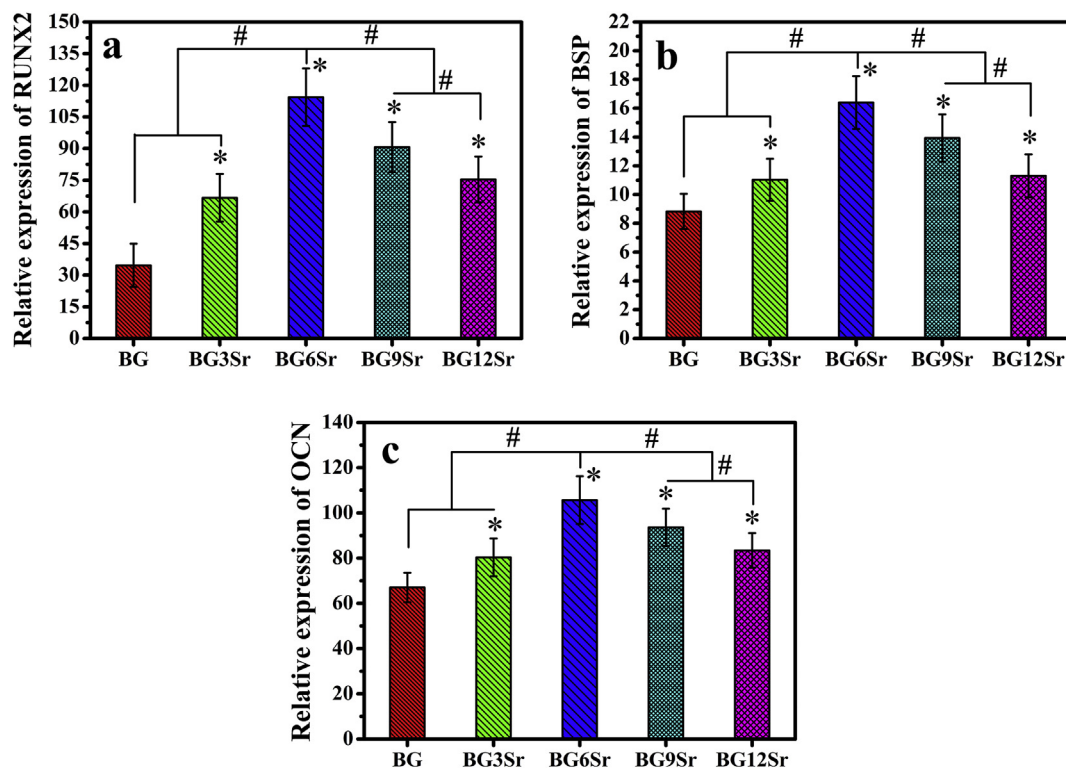


Fig. 8. Expression of early, middle and late osteogenic genes of hBMSCs. (a) Runt related transcription factor 2 (RUNX2) mRNA expression on day 7; (b) Bone sialoprotein (BSP) mRNA expression on day 14; (c) Osteocalcin (OCN) mRNA expression on day 21. Glyceraldehyde-3-phosphate dehydrogenase (GAPDH) was used as the control. (Mean ± SD; n = 5; *significant difference compared with the BG group, p < 0.05; # significant difference between groups, p < 0.05).

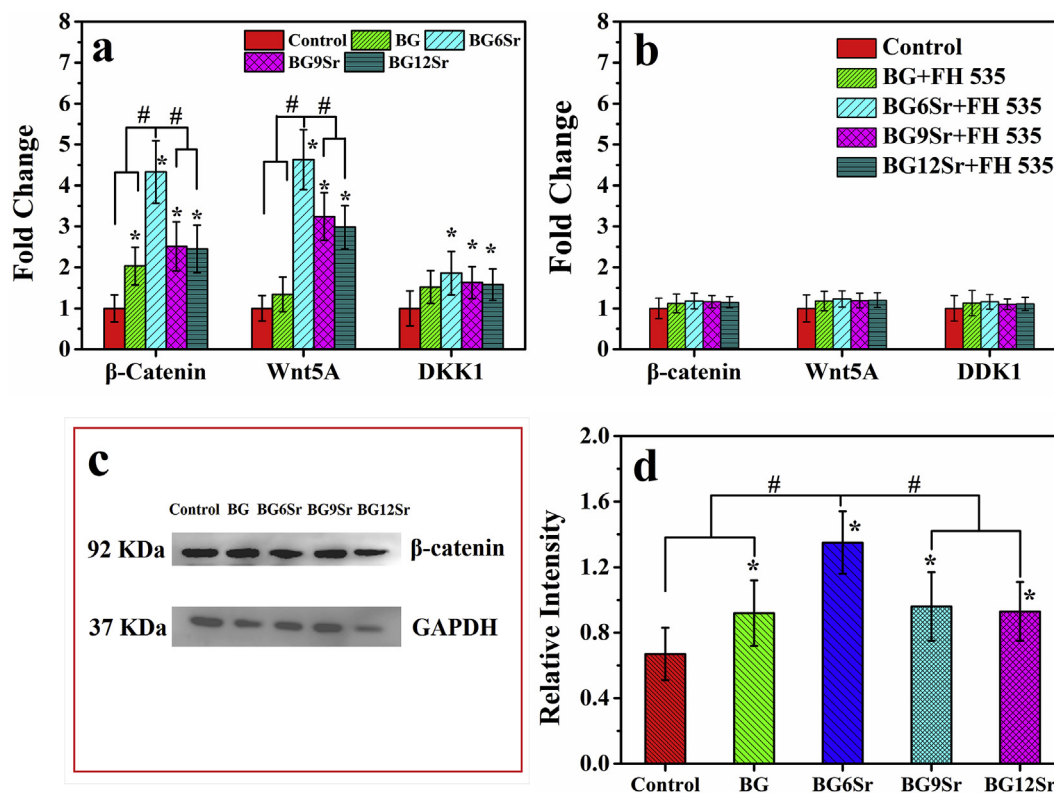


Fig. 9. (a) Wnt/β-Catenin signaling pathways related genes expression of hBMSCs cultured with borosilicate glass cements for 7 days; and (b) the same related genes expression of hBMSCs cultured with borosilicate glass cements for 7 days with FH 535 pretreated; (c) β-Catenin protein expression of hBMSCs cultured with borosilicate glass cements supplemented with osteogenic medium for 14 days by Western blot analysis; and (d) semi-quantitative statistical analysis of the gray-scale value of the straps. (Mean ± SD; n = 5; *significant difference compared with the control group, p < 0.05; # significant difference between groups, p < 0.05).

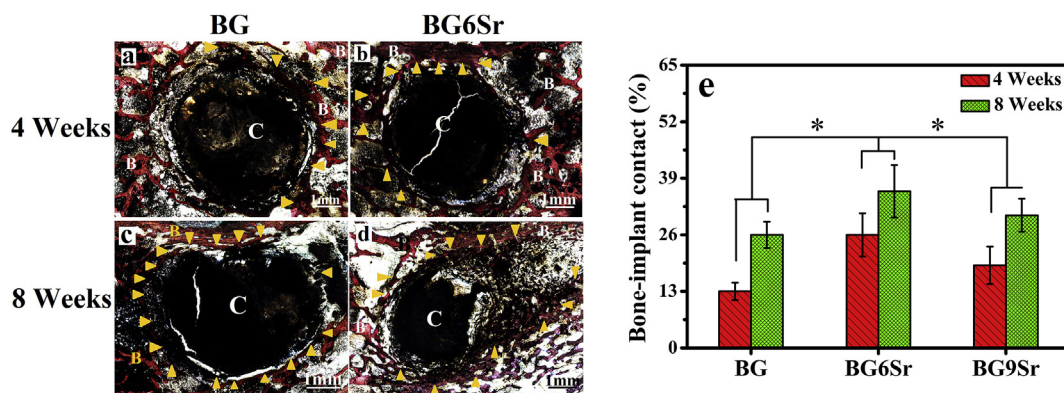


Fig. 10. (a–d) Optical images of undecalcified sections stained with van Gieson's picrofuchsin: (a, c) BG cement at 4 and 8 weeks; (b, d) BG6Sr cement at 4 and 8 weeks; new bone appears red and the cement appears black; B indicates bone, C indicates cement, and yellow arrowhead indicates new bone formation. (e) Bone–implant contact (BIC) for rabbit femoral condyle defects implanted with BG, BG6Sr and BG9Sr cements at 4 and 8 weeks postimplantation. (Mean ± SD; n = 5; *significant difference between groups, p < 0.05).

comparison, the amount of newly formed bone around the BG6Sr and BG9Sr cements appeared to be higher (yellow arrowhead) and the gaps around the cement (C) were noticeably smaller (Fig. 10b). The BIC (bone-implant contact) index for BG3Sr, BG6Sr and BG9Sr cements at 4 weeks was $13 \pm 2\%$, $26 \pm 5\%$ and $19 \pm 4\%$, respectively (Fig. 10e).

At 8 weeks, small gaps were still apparent around the BG cement (C), indicating more limited bone–cement contact (Fig. 10c). In comparison, more bone (yellow arrowhead) grew into the voids resulting from the degradation of the BG6Sr (and BG9Sr) cements (C), indicating direct bone–cement contact and better osseointegration (Fig. 10d). The BIC index for the BG3Sr, BG6Sr and BG9Sr cements was $26 \pm 3\%$, $36 \pm 6\%$ and $31 \pm 4\%$, respectively, at 8 weeks.

3.9. Microcomputed tomography (microCT) of cements implanted in vivo

MicroCT images of bone regeneration in rabbit femoral condyle defects implanted for 8 weeks with the BG, BG6Sr and BG9Sr cements are shown in Fig. 11a–f. At the interface between the bone-like graft converted from BG cement (dark gray area) and host bone (the bright area), only a smaller amount of new bone (light gray area) was formed. In comparison, there was more extensive bone formation (indicated by the red arrowhead) at the bone–cement interface for the BG6Sr and BG9Sr cements [33].

Quantitation of the micro-CT images (Fig. 11g) showed that the BMD (bone mineral density) in the defects implanted with the BG6Sr and BG9Sr cements was significantly higher than that for the BG cement

($240 \pm 43 \text{ mg cm}^{-3}$), with the BG6Sr cement showing the highest BMD value ($355 \pm 47 \text{ mg cm}^{-3}$). The BV/TV (the percent bone volume in the defects) was $68 \pm 10\%$ and $54 \pm 8\%$, respectively, for BG6Sr and BG9Sr cements which were both significantly higher than the value for the BG cement ($32 \pm 11\%$).

4. Discussion

The results showed that increasing the Sr substitution (0–12 mol % SrO) of the bioactive borosilicate glass cement resulted in a more or less continuous increase in the setting time of the cement. When the cement was immersed in PBS, an increase in Sr substitution produced a reduction in the weight loss of the cement, an increase in Sr released from the cement, and a slower formation of an HA (or HA-type) product. Sr substitution had little effect on the injectability of the cement and its compressive strength (after setting). Whereas all levels of Sr substitution used in this study enhanced the capacity of the cement to stimulate cell proliferation and function *in vitro* and to heal bone defects *in vivo*, the most significant enhancement was seen for the BG6Sr cement. Together, the results show that this BG6Sr cement can provide an optimal combination of physicochemical properties and biological performance for use as an injectable implant to heal bone defects.

4.1. Physicochemical properties of bioactive borosilicate glass cement

Increasing the Sr substitution of the bioactive borosilicate glass

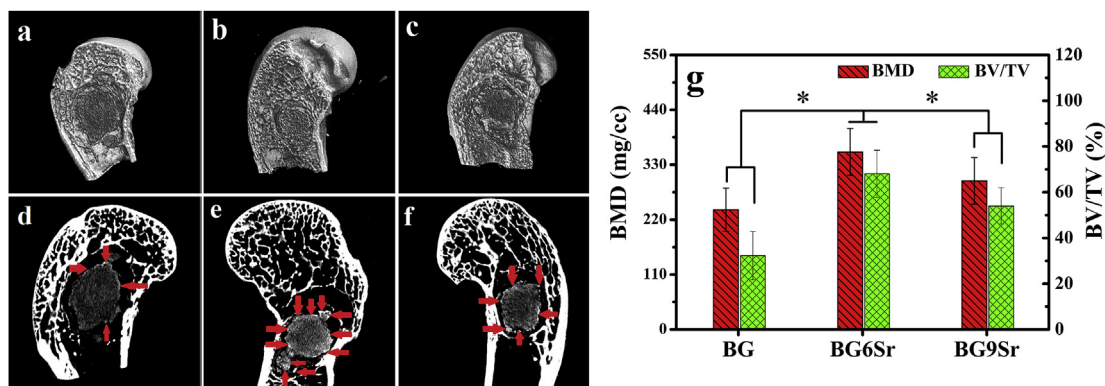


Fig. 11. (a–f) Microcomputed tomography (micro CT) images of bone regeneration in rabbit femoral condyle defects implanted for 8 weeks with borosilicate glass cements: (a, d) BG cement; (b, e) BG6Sr cement; (c, f) BG9Sr cement; The images show three-dimensional reconstructed images (a, b and c) and sagittal images (d, e and f) of the region surrounding the cement. The bright area indicates the host bone; light gray, the newly formed bone; dark gray area, the bone-like graft converted from cement; red arrowhead indicates new bone formation. (g) Bone mineral density (BMD) and bone volume/total volume (BV/TV) determined from the micro CT images. (Mean ± SD; n = 5; *significant difference between groups, p < 0.05).

cement produced a significant and continuous increase in its initial setting time, from 10.0 min for the BG cement (0 mol % SrO) to 26.3 min for the BG12Sr cement (12 mol % SrO) (Table 2). It has been reported that a desirable initial setting time of bone cements intended for clinic application is 10–25 min [34]. A setting time longer than ~25 min is undesirable because a cement paste that has not fully set can elicit a severe embolism in the surrounding tissue, especially in the vein [35,36]. Based on the potential for this adverse response, the BG12Sr cement (12 mol % SrO) may not be well suited for clinical application.

The initial setting time of the cements, as mentioned above, increased with increasing Sr substitution. Although the setting mechanism is different from that in this study, the incorporation of Sr has been observed to affect the dissolution and precipitation reactions of a calcium phosphate cement (CPC) and its setting time [35,37]. With the incorporation of 5 mol % Sr into a CPC, it was observed that the setting time increased from 4 min to more than 50 min [35,37]. In our previous study, the setting mechanism of a bioactive borosilicate glass cement (without Sr substitution) was found to involve (1) formation of an interlocking HA phase due to reaction and conversion of the borate glass particles, (2) sol to gel transition of the chitosan solution, and (3) chemical interaction between the HA phase on the converted particles and functional groups of the chitosan polymer [16]. In this study, it is unlikely that the pH-dependent sol to gel transition of chitosan would be strongly affected by the Sr substitution because there was little change in the pH when the cements were soaked in PBS (Fig. 1b). Consequently, the increase in setting time of the bioactive borosilicate glass cement used in this study may be related mainly to the formation of the HA phase and its chemical interaction with the chitosan phase [16]. Furthermore, a previous study showed that Sr substitution lowered the conversion of bioactive borosilicate glass to HA [18,19]. Conversion of the bioactive glass particles in an aqueous phosphate solution, as described earlier, involves the formation initially of ACP that subsequently crystallizes to HA. Sr ions, particularly at high concentration, have been observed to strongly inhibit the crystallization of HA [38]. Thus, a major factor responsible for the increase in the setting time with increasing Sr substitution for the bioactive borosilicate glass cement used in this study may be the slower conversion of the bioactive glass particles to HA due to the inhibitory effect of Sr [18,19].

Despite the aforementioned increase in setting time, an increase in Sr substitution had little effect on the compressive strength of the cement (Table 2). Once the cement was fully set, presumably the phases formed and the microstructural features of the cement were not very different due to the same mechanism of setting for all the cements [16]. While the compressive strength of the cements was far lower than that of human cortical bone (100–150 MPa), it was almost twice the highest strength reported for human trabecular bone (2–12 MPa) [39]. This means that the cements created in this study could be used to heal moderately-loaded and low-loaded bone [39]. In another study, Sr was observed to delay the setting of CPC (described earlier) and reduce its compressive strength after setting [40]. However, the setting mechanism of CPC is different from that of the bioactive glass cement used in this study [16,35,37,41]. For CPC, the setting mechanism was reported to involve the hydration of HA [35,37,41]. The incorporation of Sr produced a larger amount of micropores in the cement which resulted in a reduction in its compressive strength [35,37,41].

When soaked in an aqueous phosphate solution, such as PBS used in this study, bioactive borosilicate glass particles typically degraded, released ions (such as Si and B, in the form of soluble silica and borate ions, respectively, as showed in Fig. 1c) and the network modifiers (such as Na⁺, K⁺, Mg²⁺, Ca²⁺, and Sr²⁺) into the soaking medium [5–9]. While the release profile of Sr ions from the cement into PBS showed the same trend with time, the concentration of Sr released at any given time increased approximately linearly with increasing Sr substitution (Fig. 1c). This shows that the amount of Sr released from the glass at any given time can be controlled by the amount of Sr

substitution in the glass particles. For any given cement, the Sr concentration in PBS increased to a maximum value at ~20 min and decreased more slowly thereafter. The released Ca²⁺ ions can react with phosphate ions in the soaking medium to form an amorphous calcium phosphate (ACP) product that subsequently crystallizes to HA (or an HA-type material) (Figs. 2 and 3) [7,8]. This degradation and conversion into HA also resulted in a weight loss of the cements (Fig. 1a) [7,8]. As Sr can also form a phosphate material, Sr₁₀(PO₄)₆(OH)₂, that is isostructural with HA, Ca₁₀(PO₄)₆(OH)₂, a possibility is that a fraction of the Sr ions in solution was being incorporated into the HA as ACP crystallized with time [38]. This could lead to the formation of a Sr-substituted HA, such as (Ca_{1-x} Sr_x)₁₀(PO₄)₆(OH)₂ [38]. In a previous study, the release of Sr and other ions from bioactive borate glass (diameter = 0.2–3 μm) into simulated body fluid (SBF) was measured as a function of time [42]. The amount of Sr substitution in the borate glass microfibers (2 wt % SrO) was considerably smaller than those used in this study. It was found that the fibers were almost fully reacted within 2 weeks at which time 50–60% of the Sr in the fibers were released into the medium [42]. In the present study, it appears that a fraction of the Sr released from the glass remains in the PBS while the other fraction is incorporated into the HA as the ACP crystallizes. Meanwhile the strong basicity of the alkali metal and alkaline earth metal ion species (Na⁺, K⁺, Mg²⁺, Ca²⁺, and Sr²⁺) can overwhelm the weak acidic tendency of B(OH)₃ and Si(OH)₄, and finally increases the pH of soaking medium [7,8]. The pH of the PBS showed a similar trend, i.e., a more rapid increase to a maximum at ~20 min followed by slow decrease (Fig. 1b). Together, the Sr release and the pH data for all the cements indicate that after reaching its highest concentration at ~20 min, Sr ions were being removed slowly and continuously from the PBS with time.

4.2. Effect of Sr on proliferation and osteogenic differentiation of hBMSCs

The initial interaction between cells and a biomaterial involves adsorption of ions and biomolecules from the medium which is followed by adherence of cells to the adsorbed layer and subsequent spreading [26]. For a bioactive material such as bioactive glass, the ions release from the material and the nature of the adsorbed layer can strongly influence cellular response [5,43]. *In vitro* assays showed that Sr substitution of the bioactive borosilicate glass cement showed no cytotoxicity (Figs. 4 and 5), and can modulate the proliferation (Fig. 6) and function (Fig. 7) of hBMSCs incubated on the surface of the cement. Whereas Sr substitution at all levels used in this study enhanced hBMSC proliferation, ALP activity and mineralized nodule formation, the highest enhancement was observed for the BG6Sr cement (6 mol % SrO). This amount of Sr substitution in the cement also showed the best ability to upregulate early (RUNX-2), middle (BSP) and late (OCN) osteoblast marker genes (Fig. 8). These results are in accordance with previous studies that reported a stimulatory effect of Sr on osteoblastic cell behavior [20,44–46]. However, an interesting observation of this study is that there is an optimal Sr substitution of the borosilicate glass cement for stimulating hBMSC proliferation and function. Strontium ion occupies more space in the BG network, and effectively inhibits the movement and release of other ions. Therefore, borate release from the glass particles can be controlled by altering the strontium oxide content in the glass composition. This explains why different compositions of cements in this study have different effect on proliferation and osteogenic differentiation of hBMSCs cell proliferation rate [19,20]. Previous studies demonstrated that Sr ion could promote cell proliferation and osteogenesis of MSCs through Wnt/β-catenin signaling pathway [47]. Significant increase in β-catenin related mRNA and protein of hBMSCs were also detected after cultured with cement samples. However, after treated with FH 535 solution, the expression of β-catenin, DKK1, Wnt5A compared with control group was completely blocked even cultured with cement groups subsequently. Which means ion released from Sr-substituted cements may play an effect in the proliferation and

osteogenic differentiation of hMSCs through Wnt/ β -catenin signaling pathway (Fig. 9).

4.3. Effect of Sr substitution on the bone regeneration in vivo

Based on the physicochemical properties of the cements and the response of hBMSCs to the cements *in vitro*, three groups of cements, BG, BG6Sr and BG9Sr, cements were selected to evaluate their capacity to heal critical-size defects in a rabbit femur condyle model *in vivo*. Degradation of the bioactive borosilicate glass particles in the cements resulted in local release of Sr, B, Si, Na and other ions into the adjacent host bone [5,26,43]. Due to their anabolic and anticatabolic effects on the adjacent bone, Sr ions enhanced osteogenesis in the interfacial area [44–46]. Defects implanted with the BG6Sr and BG9Sr showed better peri-implant bone formation and significantly higher BMD (bone mineral density), BV/TV (bone volume) and BIC (bone–implant contact) area when compared to defects implanted with the BG cement (Figs. 10 and 11). Consistent with the results of the *in vitro* cell culture assays described earlier, the BG6Sr cement showed the best capacity to stimulate osteogenesis in the bone defects. Enhancement of osseointegration, as shown particularly by the BG6Sr cement, can be beneficial in improving implant fixation, decreasing bone resorption and promoting the formation of a stable interface [46,48]. The beneficial osteogenic effects of Sr observed in this study are also consistent with the results of previous studies which showed better bone formation due to Sr substituted HA coatings and Sr-doped HA bone graft extender [40,49–51].

In this study, the phase composition of bioactive borosilicate glass cements was not characterized as a function of implantation time *in vivo*. Although micro-CT and histomorphometric analysis showed improved osseointegration of the Sr-substituted cements, particularly the BG6Sr cement, biomechanical testing of excised specimens was not performed to determine the stability of the bone–implant interface. Future experiments will address these issues in an appropriate animal model.

5. Conclusion

Strontium (Sr) substitution of bone cements composed of bioactive borosilicate glass particles and a chitosan matrix was shown to provide an approach to modulate the physicochemical properties and osteogenic activity of the cement. An increase in Sr substitution (0–12 mol % SrO) resulted in an increase in the injectability and setting time of the cement but little change in its compressive strength. Upon immersion in PBS, the cement degraded and formed a hydroxyapatite product more slowly with increasing Sr substitution. Sr ions released from the cements modulated the proliferation, differentiation, mineralization and osteogenic-related gene expression of human bone marrow stem cells (hBMSCs) *in vitro*. Optimal enhancement of these osteogenic characteristics was achieved for a cement (designated BG6Sr) composed of glass particles substituted with 6 mol % SrO. When implanted for up to 8 weeks into rabbit femoral condyle defects *in vivo*, the BG6Sr cement supported better peri-implant bone formation and significantly higher bone–implant contact area than cements substituted with 0 or 9 mol % SrO. With local application of Sr contained bone cements, bone regeneration in rabbit femoral condyle defects was stimulated by activation of the Wnt/ β -catenin signaling pathway. These results show that the BG6Sr bone cement has a promising combination of physicochemical properties and biological performance for use as an injectable implant to heal osteoporotic fractures and bone defects.

Author contributions

Xu Cui, Yadong Zhang and Jianyun Wang, contributed to the experimental planning, performed the experiments, analyzed the data, and wrote the main manuscript text. Haobo Pan supervised the project, contributed to the experimental planning, provided funding and

intellectual input and edited the main manuscript text. Dafu Chen and Mohamed N. Rahaman supervised the project, contributed to the intellectual input and edited the main manuscript text. Deping Wang, Wenhai Huang and William W. Lu contributed to the intellectual input, scientific discussion. Chengcheng Huang, Yudong Wang, Hongsheng Yang, Wenlong Liu, Ting Wang, Changshun Ruan and Guocheng Wang contributed to the experimental planning and analyzed the data. All authors read and approved the final manuscript.

Declaration of competing interest

The authors declared that they have no conflicts of interest to this work.

Acknowledgements

This work was supported by the National Key R&D Program of China (Grant No. 2018YFC1106300 and 2017YFC1105000), the National Natural Science Foundation of China (Grant No. 51802340, 31870956, 31771041 and 81672227), the Science and Technology Project of Guangdong Province-Doctoral startup fund of 2017 (Grant No. 2017A030310318), the Frontier Science Key Research Programs of CAS (Grant No. QYZDB-SSW-JSC030), the Strategic Priority Research Program of CAS (Grant No. XDA16021000), the Shenzhen significant strategy layout project (Grant No. JCYJ20170413162104773), the Economic, Trade and information Commission of Shenzhen Municipality “Innovation and Industry Chain” (Grant No. 20170502171625936), the Beijing Municipal Natural Science Foundation (Grant No. 7161001), and Beijing Municipal Commission of Health and Family Planning (Grant No. PXM2018_026275_000001).

References

- [1] G. Fernandez de Grado, L. Keller, Y. Idoux-Gillet, Q. Wagner, A.M. Musset, N. Benkirane-Jessel, F. Bornert, D. Offner, Bone substitutes: a review of their characteristics, clinical use, and perspectives for large bone defects management, *J. Tissue Eng.* 9 (2018) 1–18.
- [2] Z.X.H. Lim, B. Rai, T.C. Tan, A.K. Ramruttan, J.H. Hui, V. Nurcombe, S.H. Teoh, S.M. Cool, Autologous bone marrow clot as an alternative to autograft for bone defect healing, *Bone Joint Res.* 8 (3) (2019) 107–117.
- [3] L. Leppik, Z.H. Han, S. Mobini, V.T. Parameswaran, M. Eischen-Loges, A. Slavici, J. Helbing, L. Pindur, K.M.C. Oliveira, M.B. Bhavsar, L. Hudak, D. Henrich, J.H. Barker, Combining electrical stimulation and tissue engineering to treat large bone defects in a rat model, *Sci. Rep.* 8 (2018) 6307.
- [4] L.L. Hench, The story of Bioglass®, *J. Mater. Sci. Mater. Med.* 17 (11) (2006) 967–978.
- [5] M.N. Rahaman, D.E. Day, B.S. Bal, Q. Fu, L.F. Bonewald, A.P. Tomsia, Bioactive glass in tissue engineering, *Acta Biomater.* 7 (6) (2011) 2355–2373.
- [6] J.R. Jones, Review of bioactive glass: from Hench to hybrids, *Acta Biomater.* 9 (1) (2013) 4457–4486.
- [7] W.H. Huang, M.N. Rahaman, D.E. Day, Y.D. Li, Mechanisms for converting bioactive silicate, borate, and borosilicate glasses to hydroxyapatite in dilute phosphate solution, *Phys. Chem. Glasses: Eur. J. Glass Sci. Technol. B.* 47 (6) (2006) 647–658.
- [8] W.H. Huang, D.E. Day, K. Kittirataniapiboon, M. N. Rahaman, Kinetics and mechanisms of the conversion of silicate (45S5), borate, and borosilicate glasses to hydroxyapatite in dilute phosphate solutions, *J. Mater. Sci. Mater. Med.* 17 (7) (2006) 583–596.
- [9] A.H. Yao, D.P. Wang, W.H. Huang, Q. Fu, M.N. Rahaman, D.E. Day, In vitro bioactive characteristics of borate-based glasses with controllable degradation behavior, *J. Am. Ceram. Soc.* 90 (1) (2007) 303–306.
- [10] Q. Fu, M.N. Rahaman, H.L. Fu, X. Liu, Silicate, borosilicate, and borate bioactive glass scaffolds with controllable degradation rate for bone tissue engineering applications. I. Preparation and in vitro degradation, *J. Biomed. Mater. Res.* 95A (1) (2010) 164–171.
- [11] Q. Fu, M.N. Rahaman, B.S. Bal, L.F. Bonewald, R.F. Brown, Silicate, borosilicate, and borate bioactive glass scaffolds with controllable degradation rate for bone tissue engineering applications. II. In vitro and in vivo biological evaluation, *J. Biomed. Mater. Res.* 95A (1) (2010) 172–179.
- [12] Y.F. Gu, W.H. Huang, M.N. Rahaman, Bone regeneration in rat calvarial defects implanted with fibrous scaffolds composed of a mixture of silicate and borate bioactive glasses, *Acta Biomater.* 9 (11) (2013) 9126–9136.
- [13] X. Zhang, T.J. Wei, Y.F. Gu, W. Xiao, X. Liu, D.P. Wang, C.Q. Zhang, W.H. Huang, M.N. Rahaman, N. Zhou, Teicoplanin-loaded borate bioactive glass implants for treating chronic bone infection in a rabbit tibia osteomyelitis model, *Biomaterials* 31 (22) (2010) 5865–5874.

- [14] X. Cui, Y.F. Gu, L. Li, H. Wang, Z.P. Xie, S.H. Luo, N. Zhou, W.H. Huang, M.N. Rahaman, In vitro bioactivity, cytocompatibility, and antibiotic release profile of gentamicin sulfate-loaded borate bioactive glass/chitosan composites, *J. Mater. Sci. Mater. Med.* 24 (10) (2013) 2391–2403.
- [15] A.J. Trias, Advancements in minimally invasive total knee arthroplasty, *Orthopedics* 26 (8) (2003) S859–S863.
- [16] X. Cui, Y.D. Zhang, H. Wang, Y.F. Gu, L. Li, J. Zhou, S.C. Zhao, W.H. Huang, N. Zhou, D.P. Wang, H.B. Pan, M.N. Rahaman, An injectable borate bioactive glass cement for bone repair: preparation, bioactivity and setting mechanism, *J. Non-Cryst. Solids* 432 (Part A) (2016) 150–157.
- [17] X. Cui, W.H. Huang, Y.D. Zhang, C.C. Huang, Z.X. Yu, L. Wang, W.L. Liu, T. Wang, J. Zhou, H. Wang, N. Zhou, D.P. Wang, H.B. Pan, M. N. Rahaman, Evaluation of an injectable bioactive borate glass cement to heal bone defects in a rabbit femoral condyle model, *Mater. Sci. Eng. C* 73 (2017) 585–595.
- [18] X. Cui, C.J. Zhao, Y.F. Gu, L. Li, H. Wang, W.H. Huang, N. Zhou, D.P. Wang, Y. Zhu, J. Xu, S.H. Luo, C.Q. Zhang, M.N. Rahaman, A novel injectable borate bioactive glass cement for local delivery of vancomycin to cure osteomyelitis and regenerate bone, *J. Mater. Sci. Mater. Med.* 25 (3) (2014) 733–745.
- [19] H.B. Pan, X.L. Zhao, X. Zhang, K.B. Zhang, L.C. Li, Z.Y. Li, W.M. Lam, W.W. Lu, D.P. Wang, W.H. Huang, K.L. Lin, J. Chang, Strontium borate glass: potential biomaterial for bone regeneration, *J. R. Soc. Interface* 7 (48) (2009) 1025–1031.
- [20] Y. Zhu, Y.M. Ouyang, Y. Chang, C.F. Luo, J. Xu, C.Q. Zhang, W.H. Huang, Evaluation of the proliferation and differentiation behaviors of mesenchymal stem cells with partially converted borate glass containing different amounts of strontium in vitro, *Mol. Med. Rep.* 7 (4) (2013) 1129–1136.
- [21] J. Buehler, P. Chappuis, J.L. Saffar, Y. Tsouderos, A. Vignery, Strontium ranelate inhibits bone resorption while maintaining bone formation in alveolar bone in monkeys (*Macaca fascicularis*), *Bone* 29 (2) (2001) 176–179.
- [22] J. Reginster, Strontium ranelate in osteoporosis, *Curr. Pharmaceut. Des.* 8 (21) (2002) 1907–1916.
- [23] S.L. Peng, G. Zhou, K.M.C. Cheung, Z. Li, W.M. Lam, Z. Zhou, W.W. Lu, Strontium promotes osteogenic differentiation of mesenchymal stem cells through the Ras/MAPK signaling pathway, *Cell. Physiol. Biochem.* 23 (1–3) (2009) 165–174.
- [24] S.L. Peng, X.S. Liu, S.S. Huang, X.L. Zhao, H.B. Pan, W.X. Zhen, K.D.K. Luk, E.X. Guo, W.W. Lu, The cross-talk between osteoclasts and osteoblasts in response to strontium treatment: involvement of osteoprotegerin, *Bone* 49 (6) (2011) 1290–1298.
- [25] P. Marie, D. Felsenberg, M. Brandi, How strontium ranelate, via opposite effects on bone resorption and formation, prevents osteoporosis, *Osteoporosis Int.* 22 (6) (2011) 1659–1667.
- [26] Y.D. Zhang, X. Cui, S.C. Zhao, H. Wang, M.N. Rahaman, Z.T. Liu, W.H. Huang, C.Q. Zhang, Evaluation of injectable strontium-containing borate bioactive glass cement with enhanced osteogenic capacity in a critical-sized rabbit femoral condyle defect model, *ACS Appl. Mater. Interfaces* 7 (4) (2015) 2393.
- [27] T. Kokubo, H. Takadama, How useful is SBF in predicting in vivo bone bioactivity? *Biomaterials* 27 (15) (2006) 2907–2915.
- [28] ISO 10993, Biological Evaluation of Medical Devices, (2018).
- [29] D.H. Zou, Z.Y. Zhang, J.C. He, K. Zhang, D.X. Ye, W. Han, J. Zhou, Y.Y. Wang, Q.L. Li, X. Liu, Y. Wang, S.J.Z. Hu, C. Zhu, W.J. Zhang, Y. Zhou, H.Y. Ao, X.Q. Jiang, Blood vessel formation in the tissue-engineered bone with the constitutively active form of HIF-1 α mediated BMSCs, *Biomaterials* 33 (7) (2012) 2097–2108.
- [30] I. Khairoun, M.G. Boltong, F.M. Driessens, J.A. Planell, Some factors controlling the injectability of calcium phosphate bone cements, *J. Mater. Sci. Mater. Med.* 9 (8) (1998) 425–428.
- [31] L. Zhao, M.D. Weir, H.H.K. Xu, An injectable calcium phosphate-alginate hydrogel-umbilical cord mesenchymal stem cell paste for bone tissue engineering, *Biomaterials* 31 (25) (2010) 65026510.
- [32] X. Liu, M.N. Rahaman, D.E. Day, Conversion of melt-derived microfibrillar borate (13-93B3) and silicate (45S5) bioactive glass in a simulated body fluid, *J. Mater. Sci. Mater. Med.* 24 (3) (2013) 583–595.
- [33] Q. Fu, W.H. Huang, W.T. Jia, M.N. Rahaman, X. Liu, A.P. Tomsia, Three-dimensional visualization of bioactive glass-bone integration in a rabbit tibia model using synchrotron X-ray microcomputed tomography, *Tissue Eng.* 17 (23 and 24) (2011) 3077–3084.
- [34] L. Chen, D. Zhai, Z.G. Huan, N. Ma, H.B. Zhu, C.T. Wu, J. Chang, Silicate bio-ceramic/PMMA composite bone cement with distinctive physicochemical and bioactive properties, *RSC Adv.* 5 (2015) 37314–37322.
- [35] G.M. Kuang, W.P. Yau, W.M. Lam, J. Wu, K.Y. Chiu, W.W. Lu, H.B. Pan, An effective approach by a chelate reaction in optimizing the setting process of strontium-incorporated calcium phosphate bone cement, *J. Biomed. Mater. Res. B* 100B (3) (2012) 778–787.
- [36] Y. Miyamoto, K. Ishikawa, M. Takechi, M. Yuasa, M. Kon, M. Nagayama, K. Asaoka, Non-decay type fast-setting calcium phosphate cement: setting behaviour in calf serum and its tissue response, *Biomaterials* 17 (14) (1996) 1429–1435.
- [37] S. Panzavolta, P. Torricelli, L. Sturba, B. Bracci, R. Giardino, A. Bigi, Setting properties and in vitro bioactivity of strontium-enriched gelatin–calcium phosphate bone cements, *J. Biomed. Mater. Res.* 84A (4) (2008) 965–972.
- [38] H.E.L. Madsen, Influence of foreign metal ions on crystal growth and morphology of brushite ($\text{CaHPO}_4 \cdot 2\text{H}_2\text{O}$) and its transformation to octacalcium phosphate and apatite, *J. Cryst. Growth* 310 (10) (2008) 2602–2612.
- [39] S.A. Goldstein, The mechanical properties of trabecular bone: dependence on anatomic location and function, *J. Biomech.* 20 (11–12) (1987) 1055–1061.
- [40] G.M. Kuang, W.P. Yau, J. Wu, K.W.K. Yeung, H.B. Pan, W.M. Lam, W.W. Lu, K.Y. Chiu, Strontium exerts dual effects on calcium phosphate cement: accelerating the degradation and enhancing the osteoconductivity both in vitro and in vivo, *J. Biomed. Mater. Res.* 103 (5) (2015) 1613–1621.
- [41] C.S. Liu, H.F. Shao, F.Y. Chen, H.Y. Zheng, Effects of the granularity of raw materials on the hydration and hardening process of calcium phosphate cement, *Biomaterials* 24 (23) (2003) 4103–4113.
- [42] X. Liu, M.N. Rahaman, D.E. Day, In vitro degradation and conversion of melt-derived Microfibrillar borate (13-93B3) bioactive glass doped with metal ions, *J. Am. Ceram. Soc.* 97 (11) (2014) 3501–3509.
- [43] A. Hoppe, N.S. Guldal, A.R. Boccaccini, A review of the biological response to ionic dissolution products from bioactive glasses and glass-ceramics, *Biomaterials* 32 (11) (2011) 2757–2774.
- [44] A. Barbara, P. Delannoy, B.G. Denis, P.J. Marie, Normal matrix mineralization induced by strontium ranelate in MC3T3-E1 osteogenic cells, *Metabolism* 53 (4) (2004) 532–537.
- [45] E. Bonnellye, A. Chabadel, F. Saltel, P. Jurdic, Dual effect of strontium ranelate: stimulation of osteoblast differentiation and inhibition of osteoclast formation and resorption in vitro, *Bone* 42 (1) (2008) 129–138.
- [46] C. Capuccini, P. Torricelli, F. Sima, E. Boanini, C. Ristoscu, B. Bracci, G. Socol, M. Fini, I.N. Mihailescu, A. Bigi, Strontium-substituted hydroxyapatite coatings synthesized by pulsed-laser deposition: in vitro osteoblast and osteoclast response, *Acta Biomater.* 4 (6) (2008) 1885–1893.
- [47] W. Zhang, D.Q. Huang, F. J. Zhao, X.L. Fu, X. Li, X.F. Chen, Synergistic effect of Strontium and Silicon in Strontium-substituted sub-micron bioactive glass for enhanced osteogenesis, *Mater. Sci. Eng. C* 89 (2018) 2445–255.
- [48] L. Maimoun, T.C. Brennan, I. Badoud, V. Dubois-Ferriere, R. Rizzoli, P. Ammann, Strontium ranelate improves implant osseointegration, *Bone* 46 (5) (2010) 1436–1441.
- [49] Y.F. Li, Q. Li, S.S. Zhu, E. Luo, J.H. Li, G. Feng, Y.M. Liao, J. Hu, The effect of strontium-substituted hydroxyapatite coating on implant fixation in ovariectomized rats, *Biomaterials* 31 (34) (2010) 9006–9014.
- [50] K. Sariibrahimoglu, W.Y. Yang, S.C.G. Leeuwenburgh, F. Yang, J.G.C. Wolke, Y. Zuo, Y.B. Li, J.A. Jansen, Development of porous polyurethane/strontium-substituted hydroxyapatite composites for bone regeneration, *J. Biomed. Mater. Res.* 103 (6) (2015) 1930–1939.
- [51] T. Matsubara, K. Suardita, M. Ishii, M. Sugiyama, A. Igarashi, R. Oda, M. Nishimura, M. Saito, K. Nakagawa, K. Yamanaka, K. Miyazaki, M. Shimizu, U.K. Bhawal, K. Tsuji, K. Nakamura, Y. Kato, Alveolar bone marrow as a cell source for regenerative medicine: differences between alveolar and iliac bone marrow stromal cells, *J. Bone Miner. Res.* 20 (3) (2005) 399–409.